INSTITUTE OF PHYSICS PUBLISHING EUROPEAN JOURNAL OF PHYSICS

Eur. J. Phys. **22** (2001) 211–218 www.iop.org/Journals/ej PII: S0143-0807(01)16759-0

Investigation of laser fundamentals using a helium–neon laser

M Jackson[1,3], D Bauen[2] and J E Hasbun[2]

[1] Department of Physics, University of Wisconsin-La Crosse, La Crosse, WI 54601, USA
[2] Department of Physics, State University of West Georgia, Carrollton, GA 30118, USA

Received 31 August 2000, in final form 30 November 2000

Abstract

Using an open-frame helium–neon (He–Ne) laser and optical spectrum analyser, students performed several upper-division laboratory experiments investigating important concepts regarding laser fundamentals. Such experiments include cavity stability (mirror geometry and thermal effects), longitudinal and transverse modes, free spectral range, and mode sweeping. In this paper we discuss, in an elementary way, the experimental procedures and results obtained.

(Some figures in this article are in colour only in the electronic version; see `www.iop.org`)

1. Introduction

The theoretical foundation for the development of the laser was laid down by Albert Einstein, who in 1917, showed that the existence of equilibrium between electromagnetic radiation and its interactions with matter required a previously undiscovered radiation process called *stimulated emission* [1]. However, his theoretical work remained largely unexploited until 1954, when Townes and co-workers developed the maser, a microwave amplifier based on the stimulated emission of radiation, see [2]. Schawlow and Townes then adapted the principle of masers to light in the visible region in 1958 [3]. In 1960, Maiman succeeded in building the first laser device, the ruby laser, that emitted a deep red light at a wavelength of 694.3 nm [4]. Within months Javan and associates developed the first gas laser, the helium–neon (He–Ne) laser, which emitted light in both the infrared (at 1.15 μm) [5] and visible (at 632.8 nm) [6] spectral regions. Since then, lasers have come to the forefront of modern technology and have been the subject of numerous investigations as well as an integral tool in a variety of experiments [7–24]. Due to its increasing importance, our respective institutions required the creation of an optics programme that included the development of upper division lecture, laboratory, and research courses. With regard to the laboratory course, in addition to the standard optics experiments in diffraction, interference, interferometers, polarization effects, etc, several experiments in laser fundamentals were introduced. These experiments were based on the work developed by Brandenberger [25] and others [26–31].

The purpose of this paper is to consolidate and review some of the previously discussed experiments and to give an overview of the topics students can investigate regarding the

[3] Author to whom correspondence should be addressed.

0143-0807/01/030211+08$30.00

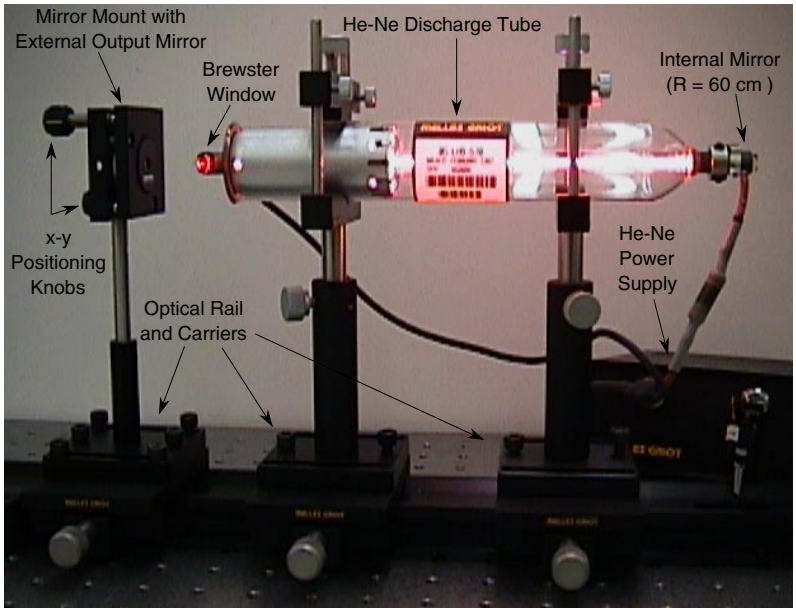

Figure 1. Open-frame He–Ne laser tube with external mirror.

fundamentals of a He–Ne laser. These topics include cavity stability, longitudinal and transverse modes, free spectral range, and mode sweeping. A brief discussion of the equipment required in the experiments discussed below will also be given.

2. Experimental details and discussion

2.1. Experiment I. Cavity stability conditions

The first experiment [25] uses a 6.0 mW He–Ne laser kit purchased from Melles Griot, model 05-LPB-670 (or the 3.5 mW version, model 05-LPB-570)[4]. This kit comes with an open frame He–Ne laser tube with a sealed Brewster window on one end and a highly reflecting (≈99.9%) 60 cm radius of curvature mirror on the other. A 45 cm radius of curvature (≈99% reflecting) output mirror along with the appropriate He–Ne laser power supply are also included. The hardware package (model 05-HBE-001) is recommended for convenience but is not required if suitable optics hardware is already available (rail, posts, mirror holders, etc). The purchase of additional output mirrors with varying curvatures (30, 60, 80, 120 cm, and ∞) is strongly recommended and will allow a thorough investigation of cavity stability.

The first step for the student is to assemble and align the system, appearing similar to figure 1. As with many optics experiments, this step is the most crucial and can take students some time to get the system properly aligned. Once aligned and lasing, students first investigate the stability of a laser cavity based on its length and mirror geometry. Depending on which output mirror is used with the system, the student can predict the cavity length requirements needed for lasing to occur (i.e. determine the regions of stability and instability) using the g-parameters [25, 32–34]

$$0 \leqslant g_1 g_2 \leqslant 1 \qquad \text{where} \qquad g_{1,2} = 1 - \frac{L}{R_{1,2}} \tag{1}$$

[4] Note this is not an endorsement of these products over others. However we have found them satisfactory and fairly easy to operate for this experiment.

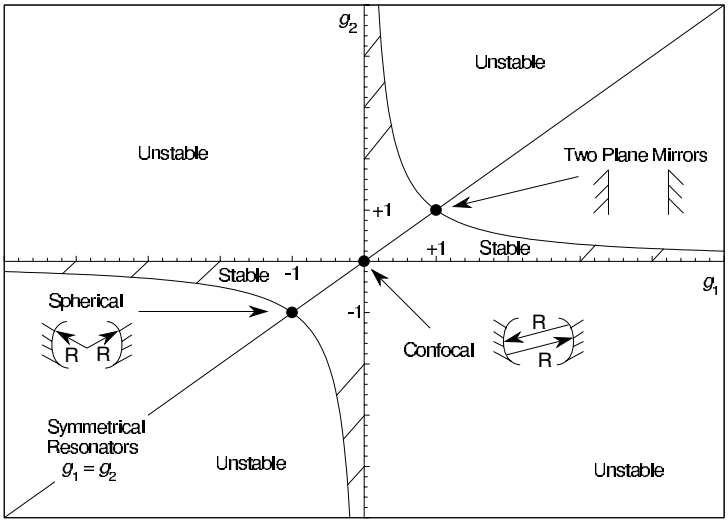

Figure 2. Resonator stability diagram. All symmetrical resonators lie along the line $g_1 = g_2$ with several special cavity configurations displayed [32, 35].

where L is the optical path length between the internal mirror and the external output mirror and $R_{1,2}$ is the radius of curvature of mirrors 1 and 2, respectively. Equation (1) is the compact form of the ray-matrix analysis for an optical cavity and is derived in such a way that, when satisfied, the ray's displacement from the optic axis is bounded, indicating that its position after a large number of round trips remains within the resonator. If equation (1) is not satisfied, then the ray's position is not bounded and it will eventually walk off the mirror and out of the resonator (which, in certain circumstances, can also be desirable). While a detailed derivation of equation (1) can be found in several texts [32, 33, 35], a graphical representation of the stability region, as illustrated in figure 2, is more convenient. Note that if the dimensions of the cavity are such that the product of the g-parameters is inside the cross-hatched region, the cavity is stable; if outside, it is unstable; and if on the border, it is conditionally stable requiring perfect alignment [32]. The insets show examples of the values for the product of g_1 and g_2 for various mirror configurations.

Students at our institutions have used each possible mirror configuration available with varying degrees of success. Figure 3 illustrates one particular example showing the normalized output power as a function of cavity length for the 45 cm output mirror. Although some cavity lengths fall within the stability region, lasing can be difficult to achieve because of less-than-perfect alignment and low output power, as illustrated in figure 3 for cavity lengths between 100 and 105 cm[5]. Even so, students have been able to achieve lasing through most of the stability region with cavity lengths as long as 150 cm, the length of our rail in this case (when using the 120 cm radius external output mirror and the 6.0 mW He–Ne laser model). This portion of the experiment can give insight into cavity design requirements regarding length and mirror curvatures, as dictated by equation (1).

2.2. Experiment II. Longitudinal and transverse modes and thermal stability

In the second experiment [25, 26, 29, 30], the cavity structure of the He–Ne laser can be investigated using an optical spectrum analyser. The 240-1 spectrum analyser and 251

[5] The only region where laser action was not achieved was in the 60–90 cm region for the 30 cm radius of curvature external mirror.

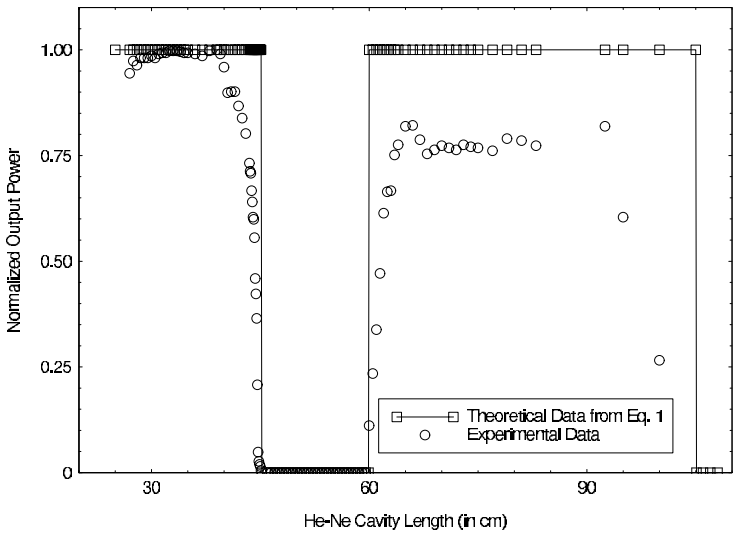

Figure 3. Normalized output power against He–Ne cavity length (in centimetres) for a 45 cm external mirror. Normalization was achieved using the maximum power reading of 4.14 mW. The theoretical curve is given for a comparison. Due to the size of the laser tube, lengths below 27 cm could not be achieved.

controller models from Coherent[6] with a free spectral range of 7.5 GHz were used[7]. For this portion of the experiment, the student must first align the spectrum analyser with the output from the He–Ne laser. Once aligned and properly adjusted for its fundamental mode, TEM_{00}, the spectrum analyser will produce an image on the oscilloscope similar to figure 4[8]. The horizontal axis is then calibrated by setting the number of horizontal divisions between adjacent modes of the spectrum analyser to its free spectral range (7.5 div at 500 μs/div is equivalent to 7.5 GHz). For our case, the calibration factor was found to be

$$\frac{\text{free spectral range of spectrum analyser}}{\text{peak separation}} = \frac{7.5\ \text{GHz}}{7.5\ \text{div} \times 500\ \mu\text{s/div}} = \frac{7.5\ \text{GHz}}{3750\ \mu\text{s}}$$
$$= 0.002\ \text{GHz}\ \mu\text{s}^{-1} = 2\ \text{MHz}\ \mu\text{s}^{-1}.$$

Next the spacing between adjacent longitudinal modes, shown in figure 5, can be measured and the free spectral range, $\Delta\nu_{\text{FSR}}$, of the laser can be calculated. In figure 5, the $\Delta\nu_{\text{FSR}}$ of the laser was measured to be about 240 MHz (1.2 div $\times$ 100 μs/div $\times$ 2 MHz μs^{-1}). The student can also predict this value using the expression [25, 28, 32–34]

$$\Delta\nu_{\text{FSR}} = \frac{c}{2L} \tag{2}$$

where L is defined as before and c is the speed of light[9]. For our situation, the cavity length was measured to be about 60.2 cm, yielding a theoretical result for $\Delta\nu_{\text{FSR}}$ of approximately 249 MHz, within 5% of the experimental value[10]. The advantage of using the Melles Griot

[6] Note this is not an endorsement of these products over others. However we have found them satisfactory and fairly easy to operate for this experiment.

[7] Although other values for the free spectral range are available, we believe the 7.5 GHz model is well suited for this experiment.

[8] Obtained using the 3.5 mW He–Ne laser model.

[9] If desired, students could also use this expression to calculate the speed of light. Using several measured values for $\Delta\nu_{\text{FSR}}$, c can usually be calculated to within 5% of its accepted value.

[10] Due to the low output power of the particular He–Ne laser used, not all of the possible longitudinal modes underneath the Doppler-broadened gain curve ($\approx$1500 MHz) were observed [34–37].

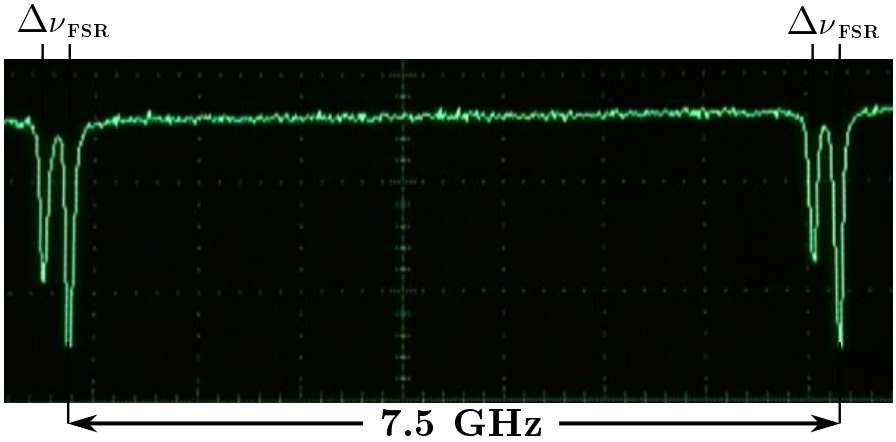

Figure 4. Observed in this scan are the adjacent modes of the spectrum analyser (separated by 7.5 GHz) as well as the adjacent longitudinal modes of the laser cavity, $\Delta\nu_{\mathrm{FSR}}$, for the 60 cm radius of curvature external output mirror. The horizontal axis of the oscilloscope was set at 500 μs/div.

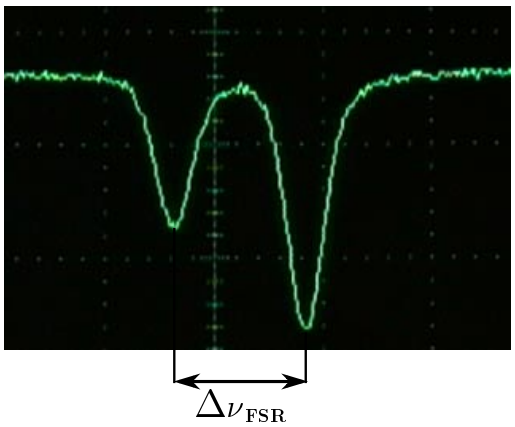

Figure 5. Close-up view for determining the free spectral range of the laser cavity with a 60 cm radius external output mirror. The horizontal axis of the oscilloscope had a setting of 100 μs/div.

laser model with an external coupling mirror in this experiment is that additional measurements with a variety of cavity lengths can easily be performed. Also, by interchanging the output mirrors, several students can uniquely perform experiments not repeated by others in the class while using the same apparatus.

In addition to longitudinal modes, students can also investigate the transverse modes of a laser cavity. By slightly adjusting the tilt of the output mirror, TEM_{qr} modes similar to those illustrated in figure 6 can easily be obtained. These modes are characterized by two integers q and r where q gives the number of minima as the beam is scanned horizontally and r is the number of minima as it is scanned vertically.

With higher-order TEM modes obtained, the transverse separation $\Delta\nu_{\mathrm{Tr}}$ between adjacent modes associated with the same longitudinal order can also be measured in the same fashion as $\Delta\nu_{\mathrm{FSR}}$. A typical scan for a TEM_{10} mode is shown in figure 7. The experimentally determined

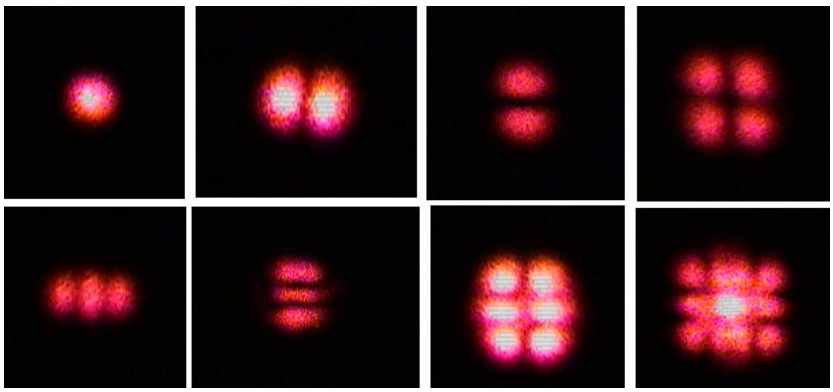

Figure 6. Various TEM modes of the He–Ne laser cavity. From left to right the modes appearing are: top row; TEM_{00}, TEM_{10}, TEM_{01}, TEM_{11}; and, bottom row; TEM_{20}, TEM_{02}, TEM_{12}, TEM_{22}.

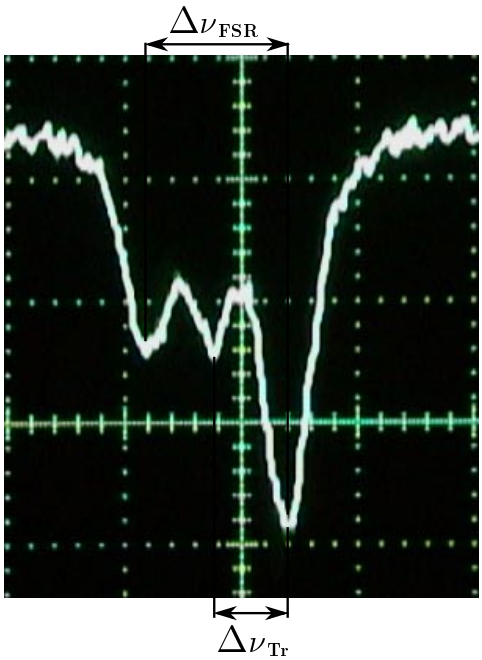

Figure 7. Observed in this scan are the adjacent longitudinal modes of the laser cavity (with the 60 cm radius external output mirror) along with a higher-order transverse mode appearing between them. This photograph was taken while the laser was producing a beam in the TEM_{10} mode with the horizontal axis of the oscilloscope set at 100 μs/div.

value can then be compared to its theoretical prediction given by [25, 28, 32–34]

$$\Delta\nu_{\mathrm{Tr}} = \frac{c}{2L}\frac{\cos^{-1}(\sqrt{g_1 g_2})}{\pi}. \tag{3}$$

As with prior measurements, agreement between experimental and theoretical values (120 and 124 MHz, respectively, for our experiment) within 5% can easily be achieved.

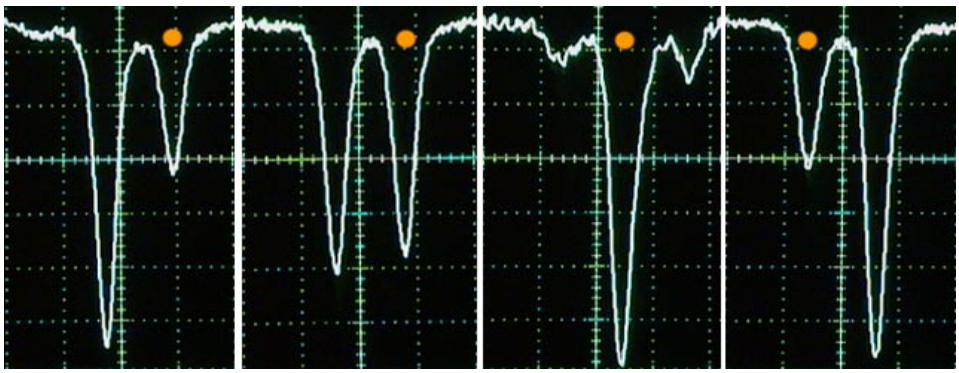

Figure 8. Consecutive photographs, with the horizonal axis set at 100 μs/div, show the mode-sweeping phenomena as the He–Ne laser is turned on. The dots show how a particular mode is swept through the gain curve.

The thermal stability of the He–Ne laser cavity and the phenomena of 'mode sweeping' can also be investigated by turning the laser off for about a minute while keeping it aligned with the spectrum analyser. Once the laser is turned back on, the laser tube begins to expand thermally. During this time, the longitudinal modes can be observed to drift through the broadened line centre, as illustrated by the successive photographs shown in figure 8. Once thermal equilibrium is reached and the laser tube has attained its equilibrium length, the mode structure becomes stable. Finally additional experiments regarding polarization, spatial coherence, gaussian beams, and speckle effects can also be investigated with this system [25, 36, 38].

3. Conclusions

The experimental procedures discussed in this work are fairly straightforward and allow for a thorough investigation of several fundamental laser concepts. In addition to providing a way to demonstrate accurately fundamental predictions from optical resonator theory, these experiments provide a hands-on approach for investigating basic laser phenomena.

Acknowledgments

The authors wish to acknowledge the financial support of Sun Microsystems, Inc. (AEG and SEIP programmes), the Faculty Development Committee and the College of Science and Allied Health, University of Wisconsin-La Crosse, the University of Wisconson-La Crosse Foundation, and the College of Arts and Science, State University of West Georgia for this work.

References

[1] Einstein A 1917 *Z. Phys.* **18** 121
[2] Gordon J P, Zeiger H J and Townes C H 1954 *Phys. Rev.* **95** 282L
[3] Schawlow A L and Townes C H 1958 *Phys. Rev.* **112** 1940
[4] Maiman T H 1960 *Nature* **187** 493
[5] Javan A, Bennett W R Jr and Herriott D R 1961 *Phys. Rev. Lett.* **6** 106
[6] White A D and Rigden J D 1962 *Proc. IRE* **50** 1697
[7] Amusia M Ya and Kornyushin Y 2000 *Eur. J. Phys.* **21** 369
[8] Lindberg A M 1999 *Am. J. Phys.* **67** 350 and references therein

[9] Umesh K S and Srinivasan K 1999 *Eur. J. Phys.* **18** 462
[10] Haag H W, Otten E W, Schick M and Weinheimer Ch 1999 *Eur. J. Phys.* **20** 231
[11] El-Zaiat S Y 1997 *Eur. J. Phys.* **18** 126
[12] Ojeda A M, Redondo E, Gonzalez Dmaz G and Martil I 1997 *Eur. J. Phys.* **18** 63
[13] Sikora P, Wiewisr P, Kowalczyk P and Radzewicz C 1997 *Eur. J. Phys.* **18** 32
[14] McKee D J, Nicholls J F H and Ruddock I S 1995 *Eur. J. Phys.* **16** 127
[15] Podoleanu A G, Taplin S R, Webb D J and Jackson D A 1994 *Eur. J. Phys.* **15** 266
[16] Ruddock I S 1994 *Eur. J. Phys.* **15** 53
[17] Moosad K P B 1989 *Eur. J. Phys.* **10** 133
[18] Eberly J H and Javanainen J 1988 *Eur. J. Phys.* **9** 265
[19] Stenholm S 1988 *Eur. J. Phys.* **9** 242
[20] Bacon M E, Johnson W J and Day M A 1986 *Eur. J. Phys.* **7** 259
[21] Harrington A P and Winter A T 1984 *Eur. J. Phys.* **5** 238
[22] Indebetouw G and Zukowski T J 1984 *Eur. J. Phys.* **5** 129
[23] von Bergmann H M and Hasson V 1980 *Eur. J. Phys.* **1** 7
[24] O'Shea D C and Peckham D C 1981 *Am. J. Phys.* **49** 915 and the references contained therein. This resource letter is an excellent source on the history of lasers and masers
[25] Brandenberger J R 1989 Laser and modern optics in undergraduate physics *Report to Foundations, Corporations, and Undergraduate Colleges* (Arlington, VA: National Science Foundation). This report is an excellent source of advanced laser experiments and is highly recommended reading
[26] Nachman P and Bernstein A C 1997 *Am. J. Phys.* **65** 202
[27] Kane D M 1991 *Am. J. Phys.* **59** 235
[28] Whitlatch N 1990 *Am. J. Phys.* **58** 556
[29] Bhatia K S 1984 *Am. J. Phys.* **52** 738
[30] Steinhaus D W 1983 *Am. J. Phys.* **51** 824
[31] Feinberg R 1982 *Am. J. Phys.* **50** 90
[32] Verdeyen J T 1995 *Laser Electronics* (Englewood Cliffs, NJ: Prentice-Hall) pp 39–44, 154–6
[33] Milonni P W and Eberly J H 1988 *Lasers* 3rd edn (New York: Wiley) pp 475–80, 495–508
[34] Siegman A E 1986 *Lasers* 1st edn (Mill Valley, CA: University Science Books) pp 462–7, 744–67
[35] Saleh B E A and Teich M C 1991 *Fundamentals of Photonics* 1st edn (New York: Wiley) pp 327–30, 480
[36] Melles Griot 1990 *Melles Griot Optics Guide 5* ch 17, 18
[37] Wilson J and Hawkes J F B 1989 *Optoelectronics: an Introduction* 2nd edn (Englewood Cliffs, NJ: Prentice-Hall) pp 176–8
[38] Mohon N and Rodemann A 1973 *Appl. Opt.* **12** 783